SHEAR LOCALIZATION IN GRANULAR AND COMMINUTED ALUMINA

H.C. Chen, M.A. Meyers, and V.F. Nesterenko*

Department of AMES, University of California, San Diego, La Jolla, CA 92093-0411

Granular alumina with two different particle sizes and densified to 85% of the theoretical value was subjected to deformation in compression by means of the radial collapse of a thick-walled cylinder. Fully dense alumina that had been pre-comminuted in a separate event was subjected to same process. The overall strains were in the 0.2-0.4 range, and the strain rate was on the order of 10^4 s^{-1}. Profuse shear localization was observed, which is interpreted in terms of hardening and softening mechanisms in the granular material. The structure of the bands for the two particle sizes (0.4 and 4 μm) was quite different, but the band thicknesses were approximately equal (10-20 μm). The comminuted alumina exhibited narrower bands (2-10 μm) developed by crack bridging.

INTRODUCTION

Viechnicki [1] divided the levels of damage in ballistic impact of ceramics into three classes: a comminuted zone produced by shock waves; radial cracks produced by the expanding stress wave; and cracks generated by the reflection of the compressive pulses at the back surface of the armor plate. In the comminuted zone, the high-amplitude shock waves create stresses that exceed the strength of ceramic. It is, as a result, finely divided into fragments. The ejection of the comminuted material from the target in order for penetration to proceed requires large deformations of the granular material. The objective of this paper is to report results of experiments especially designed to subject dense and fragmented ceramic to large "plastic" deformation at high strain rates, thus providing a new insight into the poorly understood behavior of the comminuted (or "Mescall") zone. A complete version of this work will be published elsewhere [2].

EXPERIMENTAL PROCEDURE

Alumina powders with two particle sizes (~0.4 μm and ~4 μm) and 99.97% purity were used. The densification and deformation of the aluminas were carried out using the axial collapse of a thick-walled-cylinder within which the powder was placed: this technique was developed by Nesterenko and Bondar [3] and its modification to generate controlled and prescribed shear localization in porous samples is shown in Figure 1 and described by Nesterenko et al. [4, 5]. The experimental configuration is shown in Figure 1. The process has two stages: (a) densification; (b) deformation. The alumina powder with a density of 1.5 g/cm^3 (~38% of theoretical value) was initially placed in a tubular cavity (Fig.1(a)). An explosive 1 with a low detonation velocity (3.2 km/s) was used to densify this mixture to density of 3.35 g/cm^3 (~84% of theoretical value). This stage produced mainly the densification of the powder. A cylinder hole was drilled along the longitudinal axis of copper rod and this composite cylinder was collapsed by the explosive 2 with a detonation velocity of 4.2 km/s. This second explosive event produced significant plastic deformation in the densified porous layer which resulted in profuse localized shear bands (Fig. 1(c)). For the fully dense alumina stage 1 produced comminution, and stage 2 produced deformation.

RESULTS AND DISCUSSION

The cross-sections of the collapsed ceramic cylinders are shown in Figure 2. A large number of

*On leave from Lavrentyev Institute of Hydrodynamics, Russian Academy of Sciences, Novosibirsk, 630090, Russia.

shear regions can be seen for both particle sizes. The spacing between the shear localization regions, that make an angle of 45° with the radial direction, is fairly regular, and both clockwise and counterclockwise directions are observed. The average values of internal radii r were equal to 5.9 mm after collapse for both powders. The external radii r_1 of porous layer after collapse were equal 7.3 mm and 7.4 mm for large and small particles, respectively. The initial values are 8 mm (r_0) and 9 mm (r_{10}) for both powders. The radial and tangential engineering strains (e_{rr} and $e_{\varphi\varphi}$) for the powder , assumed to be before the onset of localization are: $e_{rr} = \rho_0 / \rho - 1$ and $e_{\varphi\varphi} = \rho / \rho_0 - 1$, where ρ_0 and ρ are initial and final radii at a general point and can be calculated by Eqn. 1 (conservation of mass):

$$\rho_0^2 = \rho^2 + R_0^2 - R^2 = \rho^2 + R_{10}^2 - R_1^2 \qquad (1)$$

where R_0 (or R_{10}) and R (or R_1) are initial and final radii of inner hole (or outer cylinder surface) as shown in Fig. 1. The overall effective strain rate for the outer layer of alumina were found to be 2.5×10^4 s^{-1}, from velocity records of inner wall velocity [3-5].

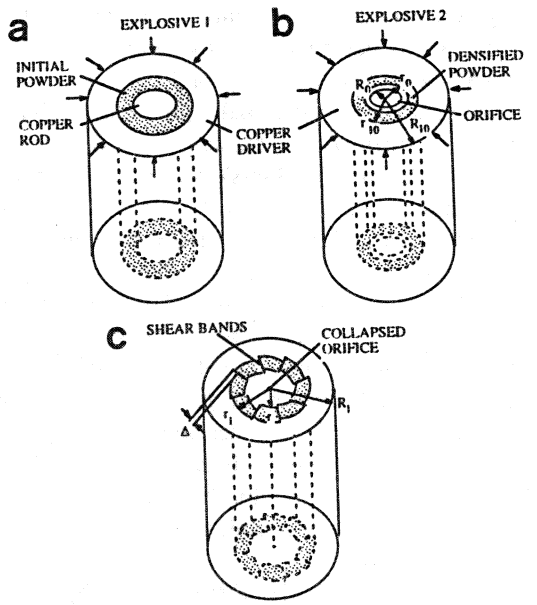

FIGURE 1. Experimental set-up: (a) configuration for densification and for comminution of bulkalumina; (b) configuration for deformation of densified alumina; (c) final configuration with schematic representation of shear localization.

The distribution of the displacements in the shear bands is depicted in Figure 3. Both distributions are close for small displacements (<50 μm), but are drastically different for larger displacements. The 0.4 μm alumina has a "tail" in the region of large displacements, which is absent for the 4 μm alumina. Figures 2 and 3 enable the conclusion that, despite of the same experimental

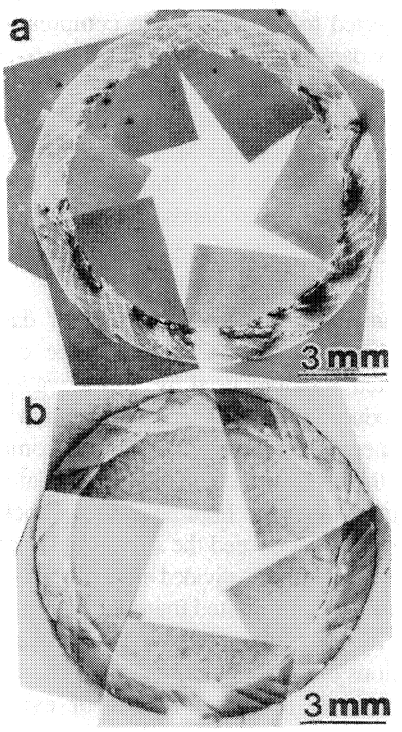

FIGURE 2. Overall view of ceramic layer after collapse process: (a) particle size ~0.4 μm; (b) 4 μm.

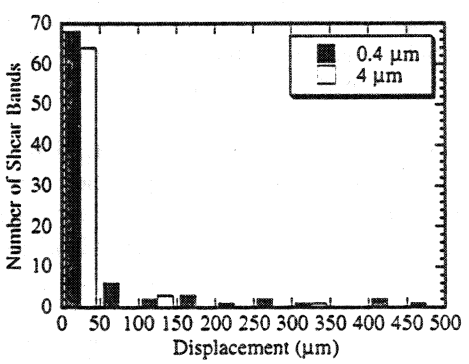

FIGURE 3. Distribution of shear bands as a function of displacement, Δ, on the outer surface of collapsed ceramic layer.

configuration for both materials, the shear-band patterning is qualitatively different. The material with "small" particles is more unstable to shear localization whereas the material with "large" particle sizes deforms uniformly with shear bands arising only at a later stage of collapse. As a consequence of a more severe loss of strength (softening) for the 0.4 μm alumina, larger displacements (Δ) tends to be produced.

The total strain imparted by the geometry, e_t, can be decomposed into the strain due to the shear bands, e_s, and homogeneous deformation, e_h ($e_t = e_h + e_s$). It is equal to -0.288. The strain due to localization is obtained by taking the tangential component of the summation of displacements, Δ, (See Fig. 1(c)). They are -0.08 and -0.033 for the small and large particle-sized materials, respectively. Thus, the homogeneous strains, e_h, are equal to -0.208 and -0.255 for the small and large particle-sized materials, respectively. Thus, localization occurs earlier for the "small" particle-sized alumina.

The shear-band structure for three displacements is shown in Fig. 4 for the 0.4 μm material. The shear-band thickness (~10-20 μm) does not depend on the displacement. As the displacement increases, cracking becomes more prominent; a central crack is seen in the shear band with largest displacement, which starts at the intermediate stage (Fig. 4(b)). Particle agglomeration is evident inside the shear band (Fig. 4). One can conclude that, as the displacement in shear band proceeds, a process of agglomeration of the ceramic occurs, providing new structural elements with typical sizes on the order of the shear band thickness.

Figure 5 shows the band for the 4 μm material at increasing displacements. It is composed of material that is clearly comminuted; the band thickness is approximately the same: 10-20 μm, considered as a scaling parameter for shear-band width in precompacted granular alumina, under high-strain-rate deformation. This behavior is in contrast with shear-band thickness in tapped granular material, without preliminary densification [6-8]. The particles show rounded edges and these features are suggestive of high temperatures and plastic flow within the particles in Fig. 5(b). At even higher displacements (Fig. 5(c)) cracking appears as a prominent feature. Regions adjacent to the cracks exhibit particle fracturing (Fig. 6).

The difference in shear-band structure between the two aluminas is a direct consequence of fracture mechanics since the flaw sizes are limited by the particle sizes. The stress required to fracture 0.4 μm particles is three times the stress required to fracture 4 μm particles ($\sigma = K_{IC}(\pi a)^{-1/2}$). This fracturing of the 4 μm particles during deformation leads to an improved repacking, which is a mechanism of deformation. Therefore, the stage of homogeneous macrodeformation is extended.

The fully dense alumina that was pre-comminuted by stage 1 exhibited primarily intergranular cracks. The particle size is dictated by the grain size. The shear bands formed in stage 2 were thinner than in the granular alumina case, with regions with clear transgranular cracks being joined by broader bands produced by, possibly, crushing and comminution of the particles, in a manner similar to the 4 μm particles (Fig.7). Thus, a shear

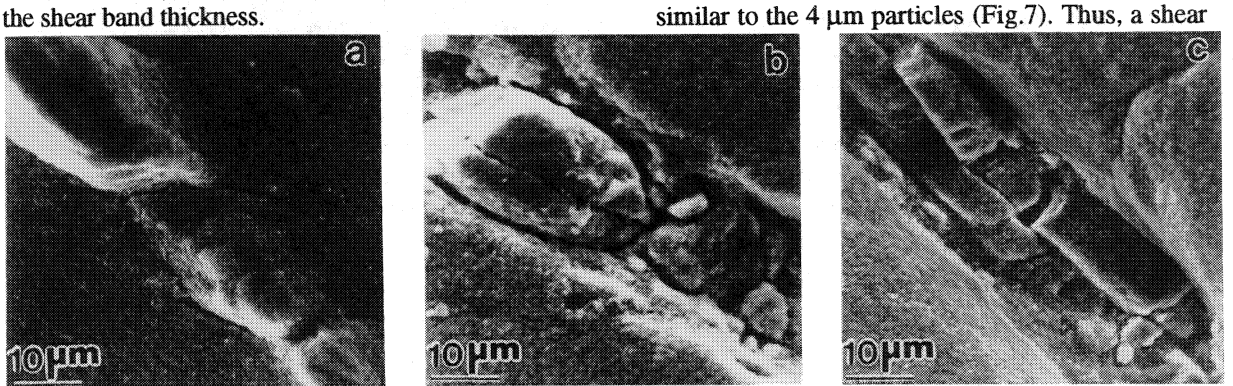

FIGURE 4. Dependence of shear band structure on displacement, Δ, in "small" particle powder: (a) Δ = 10 μm; (b) Δ = 120 μm; (c) Δ = 570 μm.

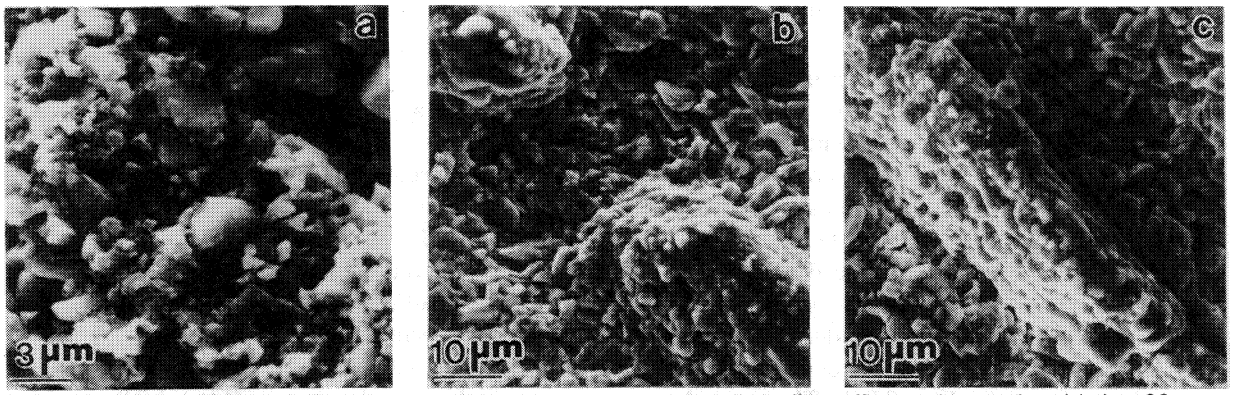

FIGURE 5. Dependence of shear band structure on displacement, Δ, in "large" particle powder: (a) Δ = 30 μm; (b) Δ = 50 μm; (c) Δ = 330 μm.

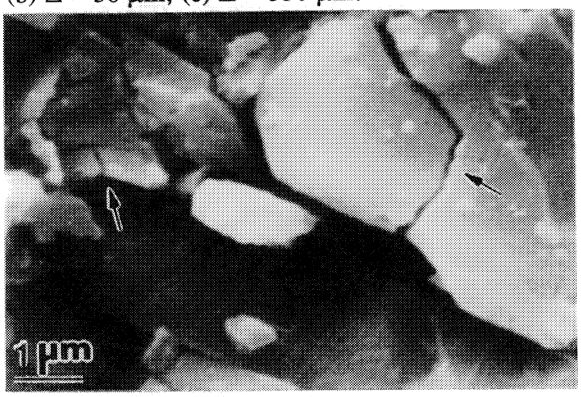

FIGURE 6. Detail of particle fracture (arrows) in regions adjacent to shear band.

crack/shear band bridging mechanism seems to be operative.

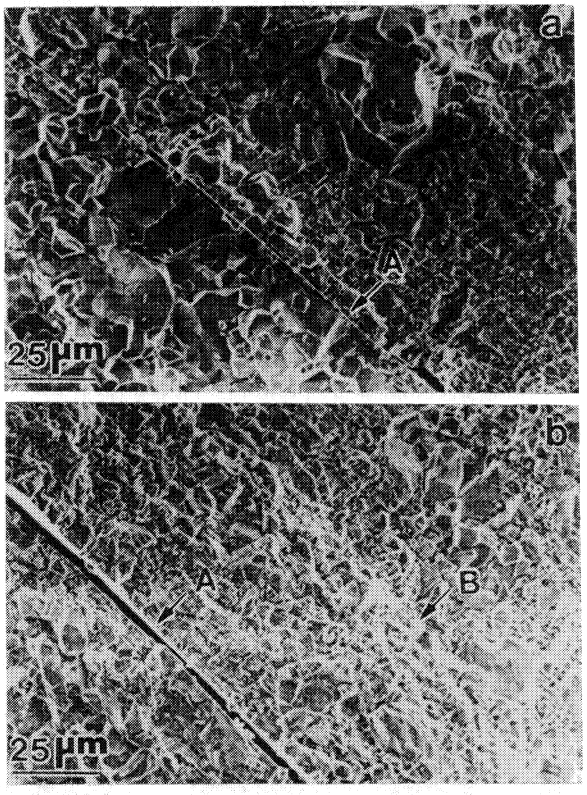

FIGURE 7. Two phenomena within shear band region: (a) shear cracks (arrows A); (b) comminuted particles adjacent to cracks (arrow B).

ACKNOWLEDGMENTS

This research was supported by the U.S. Army Research Office, Contract DAAH 04-94-G-0314, and by the U.S. Office of Naval Research, Contract N00014-94-1-1040. The help of Drs. M.P. Bondar and Ya.L. Lukyanov (Lavrentyev Institute of Hydrodynamics, Novosibirsk, Russia), in carrying out experiments, of CERALOX in donating powders, and of Dr. R.J. Clifton through discussions is gratefully acknowledged.

REFERENCES

1. D.J. Viechnicki, M.L. Slavin, and M.I. Kliman, *Cer. Bull.*, **70**, 1035 (1991).
2. V.F. Nesterenko, M.A. Meyers, and H.C. Chen, *Acta. Met. et Mat.*, to be published.
3. V.F. Nesterenko and M.P. Bondar, *DYMAT Journal*, **1**, 245 (1994).
4. V.F. Nesterenko, M.A. Meyers, H.C. Chen, and J.C.LaSalvia, *Appl. Phys. Lett.*, **65**, 3069 (1994).
5. V.F. Nesterenko, M.A. Meyers, H.C. Chen, and J.C. LaSalvia, *Met. and Mat. Trans, A*, Oct. (1995).
6. I. Vardoulakis, *Intl. J. Num. and Analyt. Meth. Geomech.*, **4**, 103 (1980).
7. H.-B. Mühlhaus and I. Vardoulakis, *Geotechnique*, **37**, 271 (1987).
8. G. Scarpelli and D.M. Wood, *Proc. IUTAM Conference on Deformation and Failure of Granular Materials, Delft*, p.473, Balkema (1982).